

# Flow feature extraction for underwater robot localization: preliminary results

Naveed Muhammad<sup>1</sup>, Nataliya Strokina<sup>2</sup>, Gert Toming<sup>1</sup>, Jeffrey Tuhtan<sup>3</sup>,  
Joni-Kristian Kämäräinen<sup>2</sup>, Maarja Kruusmaa<sup>1</sup>

**Abstract**—Underwater robots conventionally use vision and sonar sensors for perception purposes, but recently bio-inspired sensors that can sense flow have been developed. In literature, flow sensing has been shown to provide useful information about an underwater object and its surroundings. In the light of this, we develop an underwater landmark recognition technique which is based on the extraction and comparison of compact flow features. The proposed features are based on frequency spectrum of a pressure signal acquired by a piezo-resistive sensor. We report experiments in semi-natural (human-made flume with obstacles) and natural (river) underwater conditions where the proposed technique successfully recognizes previously visited locations.

**Keywords:** *flow sensing, landmark recognition, underwater robotics, bio-inspired sensors*

## I. INTRODUCTION

In order to autonomously localize and perform other useful tasks, such as object recognition and mapping, robots have to perceive their surroundings. Robots use different kinds of sensors for perceiving their environment such as cameras, sonar, lidar and radar. In underwater robotics, it has recently been discovered that flow sensing can also provide cues for perception of a robot's surroundings. The idea is biomimetic; blind cave fish for instance, despite having no vision capability at all, are able to perform navigation through complex environments using their flow sensing organ, the lateral line [1]. Introduction of flow sensing into robotics owes to the development of artificial lateral line sensors and sensor systems that can sense flow in underwater environments, such as [2], [3], [4] and [5].

Underwater robotic applications are numerous, and range from inspection of oil pipelines and ship hulls to underwater archeology. The successful incorporation of yet another sensing modality, i.e. flow sensing, can make underwater robots more robust and efficient for these applications. Incorporating flow sensing is especially beneficial in dark and visually-homogeneous underwater environments, where vision sensors do not work and sonar sensors often fail to discriminate between different objects (and hence, locations).

Autonomous localization, in mobile robotics, can be achieved with different levels of sophistication depending on the application at hand, as well as robot's sensing capability and computational power. Robot localization techniques range from *dead reckoning* i.e. simple integration of motion information over time (e.g. [6]) to *simultaneous localization*

*and mapping* or *SLAM* i.e. simultaneously creating a map and localizing oneself in an *a priori* unknown environment (e.g. [7]).

Underwater robots conventionally use vision (e.g. [8], [9]) and sonar sensors (as in [10]) for localization. Development of flow sensors for underwater robots calls for the development of techniques that can exploit flow information for robot localization. Flow-based techniques for object detection, and robot orientation estimation in laboratory conditions have been reported in literature, and are presented in the next section. But flow-based landmark recognition in semi-natural and natural environments has never been reported to the best of our knowledge. This paper presents a technique for landmark recognition in semi-natural and natural environments using a single piezo-resistive sensor. The technique is based on frequency-spectrum-based features which are extracted at different locations in an underwater environment, and later compared with newly extracted features. The technique is validated by conducting field tests in a 0.5 m wide flume and a river. In both cases, the sensor data is logged during the field experiments and the landmark recognition experiments are performed off-line.

The paper is organized as follows. Section II briefly presents some works that exploit flow sensing for robotic applications. Sections III and IV present the proposed landmark recognition technique and the results obtained during experimentation, respectively. The paper concludes in section V.

## II. FLOW SENSING IN UNDERWATER ROBOTICS

Most of the work reported on the exploitation of flow sensing for underwater robotics is oriented towards object detection and estimation of its distance from the robot, and less on robot navigation, most often only in laboratory conditions.

In the context of object detection, most common is the detection and localization of the dipole source, as in [11] and [12]. Another object detection algorithm is the detection of objects' wakes, the so called von Kármán vortex streets (KVS). KVS is a regular pattern of alternating vortices that appears behind an object in flow at moderate Reynolds numbers or when an object is moving through still or flowing water. Figure 1 shows a DPIV<sup>1</sup> image of a KVS behind a half-cylinder. From a robotic perception point of view, KVS are important because their characteristics can provide

1: Center for Biorobotics, Tallinn University of Technology, Estonia  
2: Computer Vision Group, Tampere University of Technology, Finland  
3: SJE Ecohydraulic Engineering GmbH, Germany

<sup>1</sup>Digital Particle Image Velocimetry

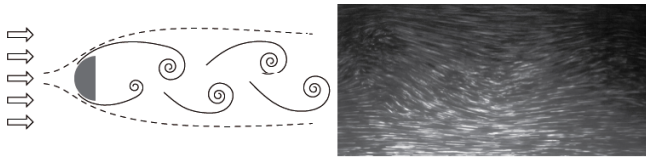


Fig. 1. Schematic of KVS behind a half-cylinder (left) and a DPIV image showing a KVS (right).

important cues about size, shape and distance of the source object (i.e. the object responsible for wake generation). Analyzing a KVS can also provide cues for estimation of robot orientation with respect to flow. For instance, [13] presents a study on time and frequency domain analysis of underwater pressure sensing data in KVS. The orientation of the platform along flow and its deviation from the center of a KVS is detected by comparing the average pressures on the right and left sides. The travel speed of vortices in KVS is detected by cross-correlating signals detected by multiple sensors on one side, while vortex shedding frequency of KVS is detected by frequency domain analysis of the recorded pressure signals. In [14] a robot can detect the presence of a KVS by applying an empirical rule to the absolute pressure measurements, and can also detect its position downstream the KVS using the pressure difference between the nose and side sensors. In [15] and [16] Bayesian filtering is employed to estimate robot orientation and flow speed using two pressure sensors (fitted one on each side). A pressure-sensor based object classification technique using PCA<sup>2</sup> is presented in [17]. It also presents the estimation of the distance of a cylindrical object with respect to a four-flow-sensor array.

#### A. Contribution

The above mentioned works on flow-sensing are limited to detection and position estimation of artificial objects with idealized shapes (usually cylinders) in laboratory conditions. In this paper we introduce first results on recognition of flows in semi-natural and natural environments obstructed by natural objects (such as stones). The technique is based on extraction and comparison of compact flow features. The proposed features are based on histograms of strength of different frequency components in a pressure signal, and are novel in that such frequency-spectrum based features have never been reported in flow-sensing-in-underwater-robotics literature. With off-line processing of field data, we show that these features can be used for recognizing landmarks (or places) that an underwater vehicles carrying a single flow sensor has already visited.

### III. APPROACH

The proposed landmark recognition technique is based on indexing, and comparison of frequency-spectrum-based features extracted from flow data. The technique comprises of the following steps:

- During the first stage, called the *learning* run, a robot is manually placed at multiple locations in an underwater environments.
- At each of these locations, feature extraction is carried out. The proposed features are 100-bin histograms of the strength of different frequency components present in the frequency spectrum of the pressure signal recorded at each location.
- The features extracted during the *learning* run constitute the *reference* feature set.
- In subsequent *test* runs, as the robot is brought back at one of the previously visited locations, a newly extracted feature is compared to the reference features. The closest match is taken as robot's current location.
  - The feature comparison is performed using  $\chi^2$  histogram distance measure.
  - The ratio of correctly classified locations to the total number of query instances during the test runs, is taken as the overall success rate of the experiment.

The following subsections describe the proposed feature definition, the feature-comparison metric, and the robot used for the experimentation.

#### A. Feature definition

The features are based on Fast-Fourier transform (FFT) of signal acquired by a single pressure sensor. Figure 2 (left) shows pressure signal acquired behind an obstacle (a cobble), at 50 Hz sampling frequency in a flume with 20 m/s flow speed, and the corresponding FFT (middle part of the figure). The presence of different frequency components in the signal depends upon several factors such as flow conditions and speed upstream from the object, size and shape of the object, etc. Since pressure is non-local, it can be seen as an integrated and simultaneous property of the flow field [18]. Thus the information contained in the pressure fluctuations contains valuable clues about the fluid environment which due to their inherent complexity are nonsimulable [19]. While the frequency spectrum of a signal acquired behind a cylinder or half-cylinder contains one strong frequency component, the significant presence of a range of frequency components in fig. 2 indicates that the object is less regularly shaped. FFT of an acquired signal therefore possesses information that can help distinguish the location at which the signal was acquired from other unique locations in an underwater environment.

We propose features that compactly encode how strongly different frequency components are present in a signal. A feature is defined as a 100-element vector with each element corresponding to regular interval (or bins) between  $L_{low}$  and  $L_{high}$ .  $L_{low}$  and  $L_{high}$  are empirical values (units in absolute FFT amplitude) and depend on the sensor and A/D interface at hand.  $L_{high}$  can be set equal to the highest absolute amplitude of a frequency component present in the flow data acquired during the learning run.  $L_{low}$  is an (above-zero) lower limit implemented to ignore the frequency components that exist with negligible amplitudes in a signal.

<sup>2</sup>Principal Component Analysis

Each element in the feature vector represents how many of the frequency components, in FFT of the flow signal, have absolute amplitude value within the corresponding interval. Corresponding to the sensor system at hand,  $L_{low}$  and  $L_{high}$  were set to 100 and 20,000 in our implementation. Figure 2 (right) shows feature extracted for the corresponding pressure signal.

### B. Feature comparison

As the features are histogram-based, a natural way of comparing the features is histogram distance. An overview of different histogram distance measures is presented in [20]. Among several intuitive choices (including Euclidean, Cosine distance, etc.)  $\chi^2$  distance was found to be the most reliable, and was therefore chosen to compare the proposed features. The chosen distance measure is defined as follows:

$$D_{\chi^2} = \sum_{i=1}^d \frac{(P_i - Q_i)^2}{(P_i + Q_i + 1)} \quad (1)$$

where  $P$  and  $Q$  are the two histograms and  $d$  is the number of histogram bins.

### C. Robotic platform

The robotic platform used for experimentation is shown in figure 3. The robot is equipped with an artificial lateral line consisting of fourteen piezo-resistive pressure sensors, seven on each side. The sensors are commercially available Intersema MS5407-AM [21]. The sensor array, via an on-board microcontroller, is connected to an external PC over a serial connection. LabVIEW<sup>3</sup> running on the external PC is used for recording pressure data as well as performing any other higher level tasks. The robot was originally developed to investigate how synchronizing the tail-beat frequency to vortices in a turbulent flow can improve swimming efficiency [22]. In the study (i.e. [22]), the vortices behind a cylinder were detected as pressure maxima, using the 14-sensor artificial lateral line.

During the experiments presented in this paper, only one (sensor no. 1 in fig. 3) of the fourteen sensors was used. The sensor, interfaced with on-board 22-bit A/D converter (MCP3553, [23]), provides pressure measurements with a sensitivity of 0.1 Pa in 0-7 bar range. Utilization of only one sensor (from the 14-sensor artificial lateral line) indicates the richness of information that can be provided by only one such sensor.

## IV. RESULTS AND DISCUSSION

The proposed features were tested for place recognition in semi-natural as well as natural environments. The following two subsections describe the experiments performed in the two types of environments and the results obtained, respectively.

### A. In semi-natural environment

Figure 4 shows the setup for the experiment in a semi-natural environment carried out at the Oskar von Miller Institute of the Technical University of Munich in Obernach, Germany. The setup consists of two obstacles placed in a flume which is fed continuously with freshly supplied river water. This outdoor laboratory facilitates experimentation under nature-like flow conditions which include natural lighting, diurnal temperature changes, and dissolved material and small amounts of suspended matter in the flumes. Two types of obstacles (cinder blocks and natural cobbles) are placed inside the flume at positions  $P3$  and  $P5$ , and a water flow of 20m/s is established in the flume. In a first *learning* run, the robot fish is manually moved through positions  $P1$ ,  $P2$ ,  $P4$  and  $P6$  with a 30 sec pressure log acquired at each location. The process of moving through the four positions and recording pressure data is then repeated, with these subsequent runs being *test* runs. Later in an off-line process, four features extracted from the *learning* run are considered as reference. The whole 30-sec log at each location is used in the FFT computation. During the localization phase, a query location and thus a query feature from a *test* run is compared with the four reference features. The closest match is taken as the robot's current location. The 0.5 m wide flume in which the experiments were conducted is shown in fig. 6. A point to be noted here is that even though computing FFT of a signal is a computationally expensive process, the processing time is just fractional on a regular PC compared to the 30 sec acquisition time which ensures that sufficient flow characteristics are captured in a signal.

In a first experiment, the middle and right object shown in fig. 5, i.e. two cobbles, were used as obstacles. As apparent from the figure, the two cobbles are fairly different in size and considerably different in shape. After performing the learning run, four test runs were recorded. Overall, a query location was correctly identified with respect to *object-1* (i.e.  $P2$ ), *object-2* (i.e.  $P4$ ) and *free flow* (i.e.  $P1$  and  $P6$ ) with a success rate of 87.5%, during the four test runs combined.

Figure 7 shows the pressure logs acquired during the learning and the 1st test run. Figure 8 shows the features extracted at the positions  $P1$ ,  $P2$ ,  $P4$  and  $P6$  during the learning and 1st test run.

The experiment was repeated by using two symmetrical and identical objects (the cinder block shown at left in fig. 5) as obstacles. As with the first experiment, one learning and four test runs were recorded. In this case intuition suggests that the features behind both the objects will be similar and the query process should confuse the two objects. It was confirmed during the experiment, as the two objects were confused during the query process one time.

### B. In natural environment

After validating the proposed technique in a semi-natural environment, an experiment was conducted in a completely natural environment i.e. river Keila, which is a lowland<sup>4</sup> river

<sup>3</sup>LabView 10.0.1, National Instruments Corporation, Austin, TX, USA

<sup>4</sup>A lowland river has a well-defined and gently flowing corridor, typically with gravelly or sandy bed.

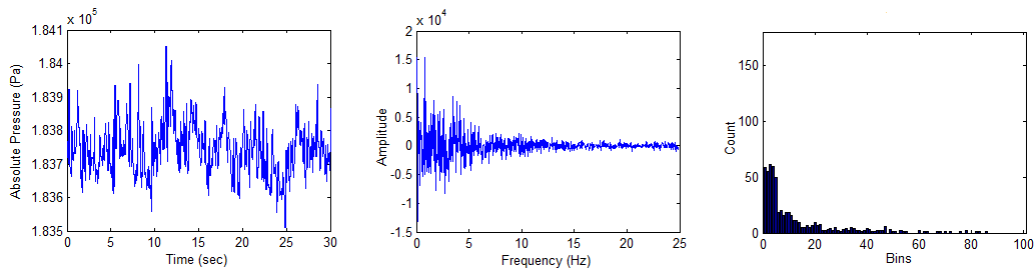


Fig. 2. Pressure signal acquired behind a cobble (left), the corresponding FFT (middle) and the extracted feature (right)

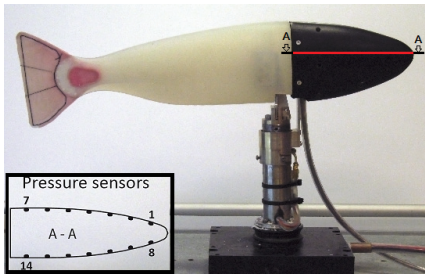


Fig. 3. The robot fish, [22].

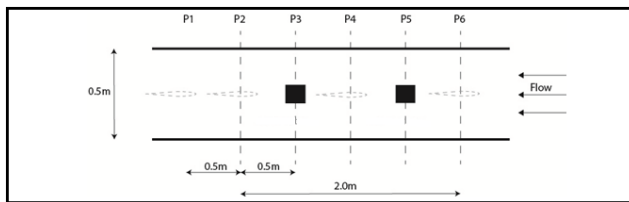


Fig. 4. Setup for localization experiments in semi-natural environment

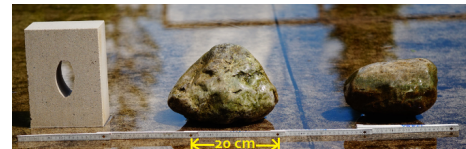


Fig. 5. Obstacles used for localization experiments in semi-natural environment.



Fig. 6. Flume used for semi-natural-environment experiments.

in Estonia. The site offers many visually dissimilar locations behind naturally occurring objects such as rocks. Four of these locations, that appeared to form a loop<sup>5</sup>, were chosen for the experiment (cf. fig. 9). In a first learning run, the robot fish was manually placed at the chosen locations *A* through *D*, recording pressure data at each location. Four reference features were computed for the four locations from the pressure data recorded during the learning run.

The robot was then placed again at positions *A* through *D* four times, corresponding to four test runs. During an off-line process, the feature extracted at each location during a test run was compared to the four reference features. For a query feature, the reference feature giving the closest match was taken as the robot's detected location out of the four reference locations. Table I shows the results for the four test runs. Over all, during the four test runs, query locations were successfully classified with respect to the four reference locations 75% of times.

### C. Discussion

1) *On the experiments in semi-natural environment:* Figure 8 shows the features extracted at the positions *P1*,

<sup>5</sup>In autonomous navigation, it can be beneficial for a robot to navigate in loops. Whenever a robot successfully identifies an already visited location, it can correct any error accumulated in its position estimate.

*P2*, *P4* and *P6* during the learning and 1st test run of the cobbles experiment. From the figure it can be noticed that the corresponding feature pairs (e.g. *P1-P1*, *P2-P2* etc.) from the two runs are visually similar.

In the experiment performed using identical cinder blocks, the query process confused the objects only one time during the four test runs. This means that the two objects were correctly identified seven times. The low confusion rate might be because of the fact that a flow feature does not only depends on the object but also on the flow conditions upstream from the object. And in this case the presence of

TABLE I  
EXPERIMENT IN NATURAL ENVIRONMENT: CORRECTLY CLASSIFIED INSTANCES IN BLUE, AND MISCLASSIFIED INSTANCES IN RED

Test run no.	Ground-truth loc.			
	A	B	C	D
1	A	C	C	D
2	A	B	C	D
3	A	B	B	C
4	A	B	C	C

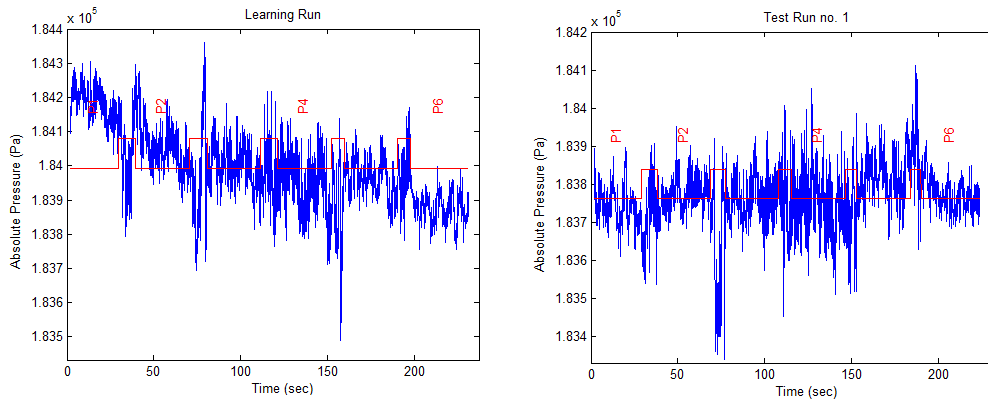


Fig. 7. Pressure log in blue, during learning (left) and the first test run (right). A red plot has been superimposed on the pressure log in order to identify different sections. A high value of the red plot represents the robot in motion, whereas a low value represents the robot being stationary. The stationary sections have also been marked with the corresponding position of the robot i.e.  $P1$ ,  $P2$ ,  $P4$  or  $P6$ .

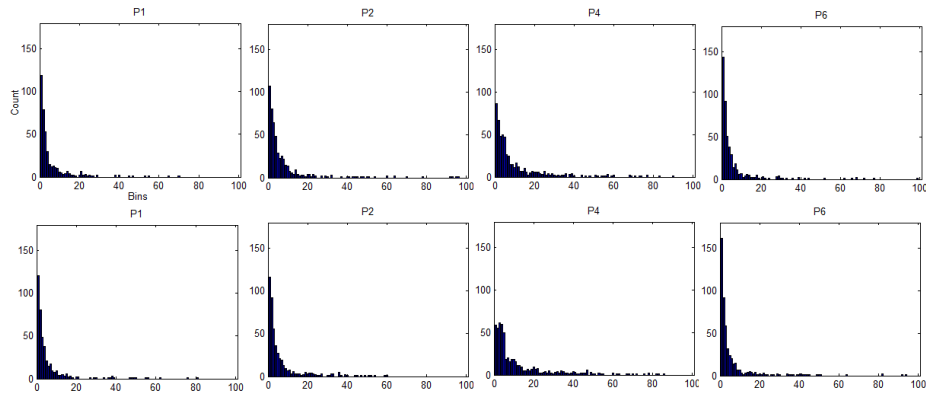


Fig. 8. FFT-based features: learning run (top), 1st test run (bottom)

an object at  $P5$  might have influenced the flow behind object at  $P3$ , even if the two objects were identical.

2) *On the experiments in natural environment:* Figure 10 shows one of the four wrong matches. The figure shows a query feature belonging to location C which was misclassified as location B. Here, it is worth mentioning that during the test runs, the robot was approximately (i.e. only by human visual judgment) placed at the locations of the learning run. The 75% success rate despite the approximate robot placement during the test runs demonstrates the soundness of the proposed technique.

## V. FUTURE WORK AND CONCLUSION

### A. Future work

As mentioned earlier, underwater robots use different techniques for localization, ranging from artificial-landmark based localization [8] to SLAM [10]. The flow-based place recognition technique, proposed in this paper, has the potential to be used in a hydrodynamic map-based localization context. A hydrodynamic map of an underwater environment can be created using the proposed features as landmarks. A robot equipped with this map can then perform autonomous map-based localization in the environment during an autonomous run. While a robot is performing SLAM, the proposed technique also has the potential to assist a vision or

sonar-based SLAM system in detecting loop closures. The significance of an independent localization layer that can assist a SLAM system to detect loop closures has already been proposed in robotics, for instance in [24]. In near future we plan to extend the proposed place recognition technique to these two scenarios, i.e. the hydrodynamic map-based localization, and loop-closure detection.

### B. Conclusion

This paper presents a technique for landmark recognition in underwater environments, using a single piezo-resistive sensor. The technique is based on extraction and comparison of compact flow features. The features are histograms of the strength of different frequency components present inside a pressure signal. The results provided in the paper show that the proposed features can be employed to recognize previously visited salient locations in semi-natural and natural environments. The success of preliminary experimentation also indicates the potential of the technique for more complicated flow-based underwater navigation scenarios such as map-based localization.

## ACKNOWLEDGMENTS

This work has been partially funded by the project FISHVIEW, that has received funding from BONUS, the

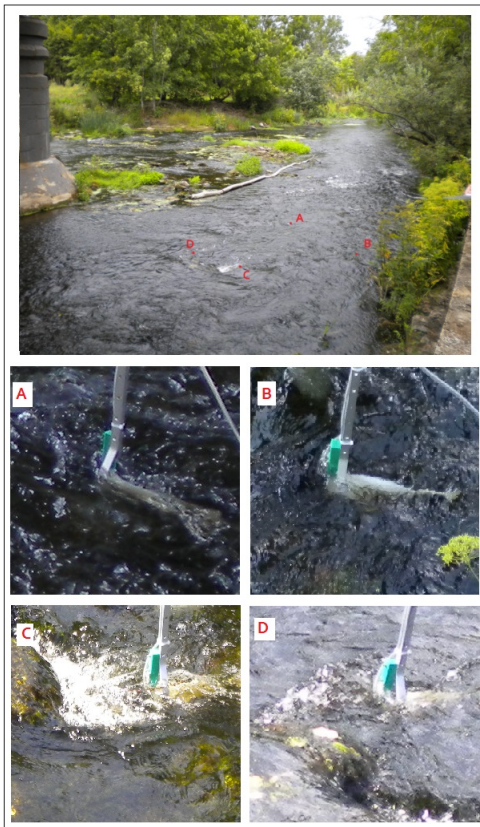


Fig. 9. Experiment in natural environment: the four locations marked by red dots were visited in order A to D. Distance between points C and D is approximately 1m.

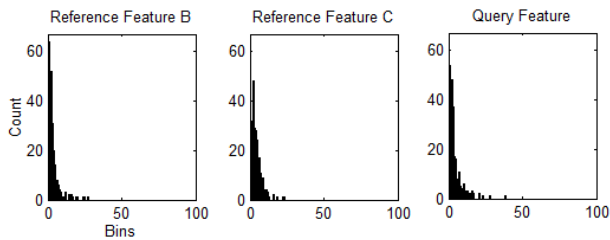


Fig. 10. One of the wrong matches in natural-environment experiment: the query feature (left) belonging to location C was misclassified as belonging to location B (reference feature shown on the right) instead of C (reference feature in the middle).

joint Baltic Sea research and development programme (Art 185), funded jointly from the European Unions Seventh Programme, Keskkonnainvesteeringute Keskus (Estonia), Forschungszentrum Jlich Beteiligungsgesellschaft mbH (Germany) and Academy of Finland.

The authors would like to thank Prof. Peter Rutschmann and Mathilde Cuchet of the Oskar von Miller Institute for their generous facilitation of the experiments in Obernach.

#### REFERENCES

[1] A. Gao and M. Triantafyllou, "Bio-inspired pressure sensing for active yaw control of underwater vehicles," in *Oceans*, October 2012.  
 [2] A. Quattieri, F. Rizzi, G. Epifani, A. Ernits, M. Kruusmaa, and M. D. Vittorio, "Parylene-coated bioinspired artificial hair cell for liquid flow sensing," *Microelectronic Engineering*, vol. 98, pp. 516–519, October 2012.

[3] A. M. K. Dagamesh, C. Bruinink, H. Droodendink, R. J. Wiegerink, T. S. J. Lammerink, and G. J. M. Krijnen, "Engineering of biomimetic hair-flow sensor arrays dedicated to high-resolution flow field measurements," in *IEEE Sensors*, November 2010.  
 [4] Y. Yang, J. Chen, J. Engel, S. Pandya, N. Chen, C. Tucker, S. Coombs, D. L. Jones, and C. Liu, "Distant touch hydrodynamic imaging with an artificial lateral line," *Proceedings of National Academy of Sciences of the United States of America*, vol. 103, 2006.  
 [5] A. G. P. Kottapalli, M. Asadina, J. M. Miao, G. Barbastathis, and M. S. Triantafyllou, "A flexible liquid crystal polymer mems pressure sensor array for fish-like underwater sensing," *Smart Materials and Structures*, vol. 21, 2012.  
 [6] D. Sekimori and F. Miyazaki, "Precise dead-reckoning for mobile robots using multiple optical mouse sensors," *Informatics in Control Automation and Robotics II*, pp. 125–151, 2007.  
 [7] M. Cummins and P. Newman, "Fab-map: Probabilistic localization and mapping in the space of appearance," *International Journal of Robotics Research*, vol. 27, no. 6, pp. 647–665, 2008.  
 [8] M. Carreras, P. Ridao, R. Garcia, and T. Nicosevici, "Vision-based localization of an underwater robot in a structured environment," in *IEEE International Conference on Robotics and Automation*, Taipei, Taiwan, September 2003.  
 [9] N. Palomeras, S. Nagappa, D. Ribas, N. Gracias, and M. Carreras, "Vision-based localization and mapping system for auv intervention," in *MTS/IEEE OCEANS*, Bergen, June 2013.  
 [10] D. Frouher, J. Hartmann, M. Litza, and E. Maehle, "Sonar-based fastslam in an underwater environment using walls as features," in *15th International Conference on Advanced Robotics*, June 2011, pp. 588–593.  
 [11] N. Chen, C. Tucker, J. M. Engel, Y. Yang, S. Pandya, and C. Liu, "Design and characterization of artificial hair sensor for flow sensing with ultrahigh velocity and angular sensitivity," *Journal of Microelectromechanical Systems*, vol. 16, pp. 999–1014, 2007.  
 [12] S. Peleshanko, M. D. Julian, M. Ornatska, M. E. McConney, M. C. LeMieux, N. Chen, C. Tucker, Y. Yang, C. Liu, J. A. C. Humphrey, and V. V. Tsukruk, "Hydrogel-encapsulated microfabricated hair mimicking fish cupula neuromast," *Advanced Materials*, vol. 19, pp. 2903–2909, 2007.  
 [13] R. Venturelli, O. Akanyeti, F. Visentin, J. Jezov, L. Chambers, G. Toming, J. Brown, M. Kruusmaa, W. M. Megill, and P. Fiorini, "Hydrodynamic pressure sensing with an artificial lateral line in steady and unsteady flows," *Bioinspiration and Biomimetics*, vol. 7, 2012.  
 [14] T. Salumae and M. Kruusmaa, "Flow-relative control of an underwater robot," *Proceedings of the Royal Society A*, vol. 469, pp. 1–19, 2013.  
 [15] L. DeVries and D. Paley, "Observability-based optimization for flow sensing and control of an underwater vehicle in a uniform flowfield," in *American Control Conference*, June 2013, pp. 1386–1391.  
 [16] F. D. Lagor, L. D. DeVries, K. M. Waychoff, and D. A. Paley, "Bio-inspired flow sensing and control: Autonomous underwater navigation using distributed pressure measurements," in *18th International Symposium on Unmanned Untethered Submersible Technology*, Portsmouth, NH, USA, August 2013.  
 [17] V. I. Fernandez, A. Maertens, F. M. Yaul, J. Dahl, J. H. Lang, and M. S. Triantafyllou, "Lateral-line-inspired sensor arrays for navigation and object identification," *Marine Technology Society Journal*, vol. 45, pp. 130–146, 2011.  
 [18] P. Davidson, *Turbulence: An Introduction for Scientists and Engineers*. Oxford University Press, 2004.  
 [19] J. A. Tuhtan, M. Kruusmaa, M. Schneider, G. Toming, and I. Kopecki, "Fishview: Developing a hydrodynamic imaging system using a robot fish with an artificial lateral line," in *10th International Symposium on EcoHydrolics*, Trondheim, Norway, June 2014.  
 [20] S.-H. Cha, "Taxonomy of nominal type histogram distance measures," in *American Conference on Applied Mathematics*. World Scientific and Engineering Academy and Society (WSEAS), 2008, pp. 325–330.  
 [21] *MS54XX Miniature SMD Pressure Sensor*, Measurement Specialties, 45738 Northport Loop West, Fremont, CA 94538, USA.  
 [22] J. Jezov, O. Akanyeti, L. D. Chambers, and M. Kruusmaa, "Sensing oscillations in unsteady flow for better robotic swimming efficiency," in *IEEE International Conference on Systems, Man, and Cybernetics*, Seoul, Korea, October 2012.  
 [23] *MCP3553*, Microchip Technology Inc., Chandler, Arizona, USA.  
 [24] A. Angeli, D. Filliat, S. Doncieux, and J.-A. Meyer, "Fast and incremental method for loop-closure detection using bags of visual words," *IEEE Transactions on Robotics*, vol. 24, no. 5, pp. 1027–1037, October 2008.